

# Preparation and characterization of Pt-promoted NiY and CoY catalysts employed for 4-nitrophenol reduction

Zeinhom M. El-Bahy<sup>a,b,\*</sup>

<sup>a</sup> Chemistry Department, Faculty of Science, Taif University, Taif, Saudi Arabia

<sup>b</sup> Chemistry Department, Faculty of Science, Al-Azhar University, Nasr City 11884, Cairo, Egypt



## ARTICLE INFO

### Article history:

Received 24 May 2013

Received in revised form 24 August 2013

Accepted 26 August 2013

Available online xxx

### Keywords:

4-Nitrophenol

Reduction

4-Aminophenol

NaY zeolite

Platinum

## ABSTRACT

The reduction of 4-nitrophenol (4-NP) by NaBH<sub>4</sub> was used as a probe reaction to investigate the promotion effect of platinum to CoY and NiY catalysts. Subsequent catalysts preparation by ion exchange method, they were characterized by XRD, FTIR, TEM, EXD and surface area measurements at -196 °C. The metal particle size calculated from XRD patterns and TEM images was ≈20 nm for PtY and ≈8–14 nm for Pt-promoted CoY and NiY catalysts. The catalytic efficiency toward the hydrogenation reaction was in the order of PtY < NiY < CoY < PtNiY < PtCoY. Using Pt-promoted CoY catalyst, the reaction rate of 4-NP reduction at 28 °C was found to be 54 times higher than that of PtY catalyst. Moreover, after reduction of the employed catalysts, a significant improvement in the catalytic performance was observed toward the hydrogenation reaction. The specific rate constant of the hydrogenation reaction in the presence of reduced PtCoY was 3.7, 50 and 201 times more than that in the presence of unreduced PtCoY, CoY and PtY catalysts, respectively. Both of the catalysts promotion with platinum and their reduction extremely decreased the apparent activation energy ( $E_a$ ), whereas it decreased in case of reduced PtCoY to ≈one third of its value in case of PtY. The catalytic activity was found to have a logarithmic relation with the catalyst mass.

© 2013 Elsevier B.V. All rights reserved.

## 1. Introduction

Faujasite zeolites have many potential properties with their novel cage structure, high surface area and their high affinity for adsorption of enormous reactants and products while being used as supports for catalysts in several reactions. Precious metals-loaded faujasite zeolites have attracted much attention as they are interesting host-guest materials. Specifically, it is of interest to investigate the activity of platinum supported on NaY zeolite for the development of these catalysts for the industrial applications of organic pollutants removal by hydrogenation reactions. Bimetallic platinum with a second metal such as PtFe/Al<sub>2</sub>O<sub>3</sub> [1], PtCo/Al<sub>2</sub>O<sub>3</sub> [2], supported PtNi [3,4], and Pt-Cr/ZSM-5 [5] have been prepared using different preparation methods such as successive impregnation, incipient wetness and competitive ion exchange methods. They have been used in some reactions such as CO oxidation, isomerization reactions and alkane conversion. Although, the interaction between the noble metals and the zeolitic structure can lead to the generation of electronic deficient sites which have high activity toward hydrogenation reactions, seeking of higher activity

and cheaper cost catalysts never ends. The presence of transition metal as a second element (d electrons are available) can increase the Pt electronic density and, consequently, enhance the catalytic activity [5]. In the previous oxide promoted catalysts, the activity is likely to be controlled via the Pt-promoter interface and so it is essential that the oxide and Pt should be associated together to increase the catalytic activity [6] with high dispersion. Such dispersion is difficult to be achieved by traditional preparation methods such as impregnation, incipient wetness or co-precipitation. One of the ways to attain high dispersion is to use ion exchange method which can homogeneously distribute ions on the surface. In a previous work [7], we used successive ion exchange method to prepare PtFeY catalyst and study its catalytic activity toward CO oxidation. As far as we know, Pt was not used as promoter to CoY and NiY catalysts using ion exchange method. Therefore, it will be interesting to use such method to prepare Pt-promoted CoY and NiY catalysts and investigate their catalytic activity toward the removal of hazardous materials.

Upgrading water quality is getting more interest with increasing the industrial applications. Phenolic compounds are considered as priority pollutants since they are harmful to organisms even at low concentrations [8,9]. Among various phenolic compounds, 4-nitrophenol (4-NP) is one of the frequently occurring by-products, which is toxic to the environment. On the other hand, 4-NP is

\* Corresponding author. Tel.: +20 224129790.

E-mail addresses: [zeinelbahy2020@yahoo.com](mailto:zeinelbahy2020@yahoo.com), [zeinelbahy2020@hotmail.com](mailto:zeinelbahy2020@hotmail.com)

reduced to form 4-aminophenol (4-AP) which has great commercial importance as an intermediate for the preparation of analgesic and antipyretic drugs [10–12]. In view of the hazardous effect of 4-NP and the growing demand for 4-AP, direct catalytic reduction of the former to the later becomes important.

$\text{NaBH}_4$  has the potential to be a useful hydrogen storage compound ( $\text{NaBH}_4 + 2\text{H}_2\text{O} \rightarrow \text{NaBO}_2 + 4\text{H}_2$ ). The speed of releasing of hydrogen can be raised by adding metal containing catalysts [13]. Reduction of 4-NP with  $\text{NaBH}_4$  in the aqueous medium is kinetically inert reaction, and generally it occurs in the presence of metal containing catalysts such as colloids of platinum nanoparticles [14,15].

Reduction of 4-NP to 4-AP with an excess amount of  $\text{NaBH}_4$  has often been used as a model reaction to examine the catalytic performance of metal nanoparticles [16]. It has been extensively studied involving various noble metal nanocatalysts such as Au, Ag, Pt and Pd [17]. Compared with Au, Pt, Pd and Ag cobalt and nickel are not expensive. Moreover, they can be used as binary metallic system with precious metals such as Pt to enhance its activity. Based on our literature survey, the use of Pt-promoted CoY and NiY catalysts for the 4-NP reduction has not been reported. So, employing these catalysts for such reaction is interesting in view point of applied and industrial importance.

The apparent lesser reports on the metal oxides-promoted PtY catalyst for the 4-NP reduction hearten the author to prepare Pt-promoted CoY and NiY catalysts using successive ion exchange method and characterize the prepared catalysts with different techniques. The catalysts will be employed in the reduction of the hazardous organic pollutant 4-NP to form the useful 4-AP.

## 2. Experimental

### 2.1. Catalyst preparation

All the employed reagents in this study were of analytical grade. To prepare platinum, cobalt and nickel supported NaY solids, 4 g of NaY zeolite (Toyota Company Ltd., Japan. CBV, SAR=5.1) were soaked in 0.01 M solution of  $\text{Pt}(\text{NH}_3)_4\text{Cl}_2 \cdot \text{H}_2\text{O}$  (Mitsuwa's Pure Chemicals),  $\text{Ni}(\text{NO}_3)_2 \cdot 6\text{H}_2\text{O}$  and  $\text{Co}(\text{NO}_3)_2 \cdot 6\text{H}_2\text{O}$  (Aldrich), respectively. The mixtures ( $\text{pH} \approx 6.2$ ) were stirred for 24 h at room temperature, and then the solution was filtered off. This was repeated three times to increase the degree of ion exchange. After filtration, the suspensions were washed with de-ionized water, dried, and finally calcined at 500 °C in air for 3 h. The resulted solids were inferred as PtY, CoY and NiY for platinum, cobalt and nickel supported NaY zeolite, respectively.

The binary systems PtCo and PtNi catalysts supported on NaY zeolite were prepared by successive ion exchange method. In two separated beakers, 2 g of the previously prepared powders CoY and NiY were added to 0.01 M of  $\text{Pt}(\text{NH}_3)_4\text{Cl}_2 \cdot \text{H}_2\text{O}$  solution at pH 10. Then, the mixtures were stirred at 80 °C for 1 h, filtered, washed with distilled water, dried at 100 °C for 24 h and finally calcined at 500 °C for 3 h. The obtained solids were referred as PtCoY and PtNiY for Pt-promoted CoY and NiY catalysts, respectively.

### 2.2. Catalyst characterization

The parent NaY and the prepared catalysts were characterized by various techniques such as X-ray diffraction (XRD), FTIR, surface texture parameters measurements, TEM and elemental analysis by EDX technique.

XRD patterns of parent NaY and the prepared samples were collected at room temperature with an X-ray diffractometer, D8 Advance (Bruker axs), with a Cu K $\alpha$  radiation source (30 kV and 20 mA) in the  $2\theta$  range of 5–60°. Hall-equation–Scherer's formula  $D = 0.9\lambda/\beta \cos \theta$  [18] was used to determine the average crystallite

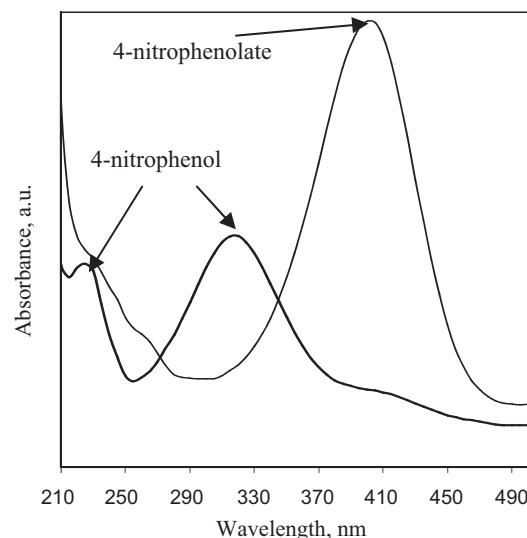


**Fig. 1.** UV-vis absorption spectra for the change of 4-NP to 4-AP in the presence of  $\text{NaBH}_4$ .

size ( $D$ ) of the obtained powders; where  $\lambda$  represents the X-ray wavelength (1.54 Å),  $\theta$  is the Bragg's angle and  $\beta$  (in radians) is the pure full width of the fraction line at half of the maximum capacity.

IR spectra were recorded in the solid state as KBr pellet on JASCO FTIR-600 Plus with a spectral resolution of 2 cm<sup>-1</sup> and accumulation of 100 scans at room temperature.

$\text{N}_2$  adsorption–desorption isotherms were used to examine the porous properties of each sample by using nitrogen as the adsorbent at –196 °C. The measurements were carried out in a Quantachrome AS1Win. (Quantachrome instruments Version 2.01). Before analysis, all samples were pretreated in vacuum at 300 °C for 2 h. The surface area was calculated using the Brunauer–Emmett–Teller (BET) method based on adsorption data in the partial pressure ( $P/P_0$ ) range of 0.02–0.25. The total pore volume was determined from the amount of nitrogen adsorbed at  $P/P_0 = \text{ca. } 0.95$ . Pore size and pore volume were obtained via *t*-plot analysis of the isotherm data.

Transmission electron microscope (TEM) micrographs of the prepared catalysts were measured using JEOL JEM-1010 transmission electron microscope at an accelerating voltage of 60 kV. Samples were previously ground and ultrasonically dispersed in water. The solids were then deposited over a thin carbon film supported on a standard copper grid.

EDX analysis of the prepared samples was accomplished to estimate the weight ratio (wt%) of the metal ions by using an X-ray energy dispersive spectroscopy (JOEL, Model: JSM-5600, Japan).

### 2.3. Catalytic reduction of 4-nitrophenol

The performance of 4-NP reduction in the presence of  $\text{NaBH}_4$  was investigated in batch mode. Typically, 100 ml aqueous solution of 4-NP (0.72 mmol) was mixed with  $\text{NaBH}_4$  (1.5 mmol) as a reducing agent. The concentration of the  $\text{NaBH}_4$  was chosen to exceed the concentration of the 4-NP by far. It is known that the light yellow 4-NP exhibits a strong absorption peak at 317 nm (Fig. 1), however, after addition of  $\text{NaBH}_4$  to its aqueous solution (increase of alkalinity), 4-nitrophenolate ions (dark yellow) are formed with a new absorption band at 400 nm [19–21].



The temperature of the mixture (4-NP +  $\text{NaBH}_4$ ) was kept constant at the desired temperature using water bath ( $t \pm 1^\circ\text{C}$ ) and

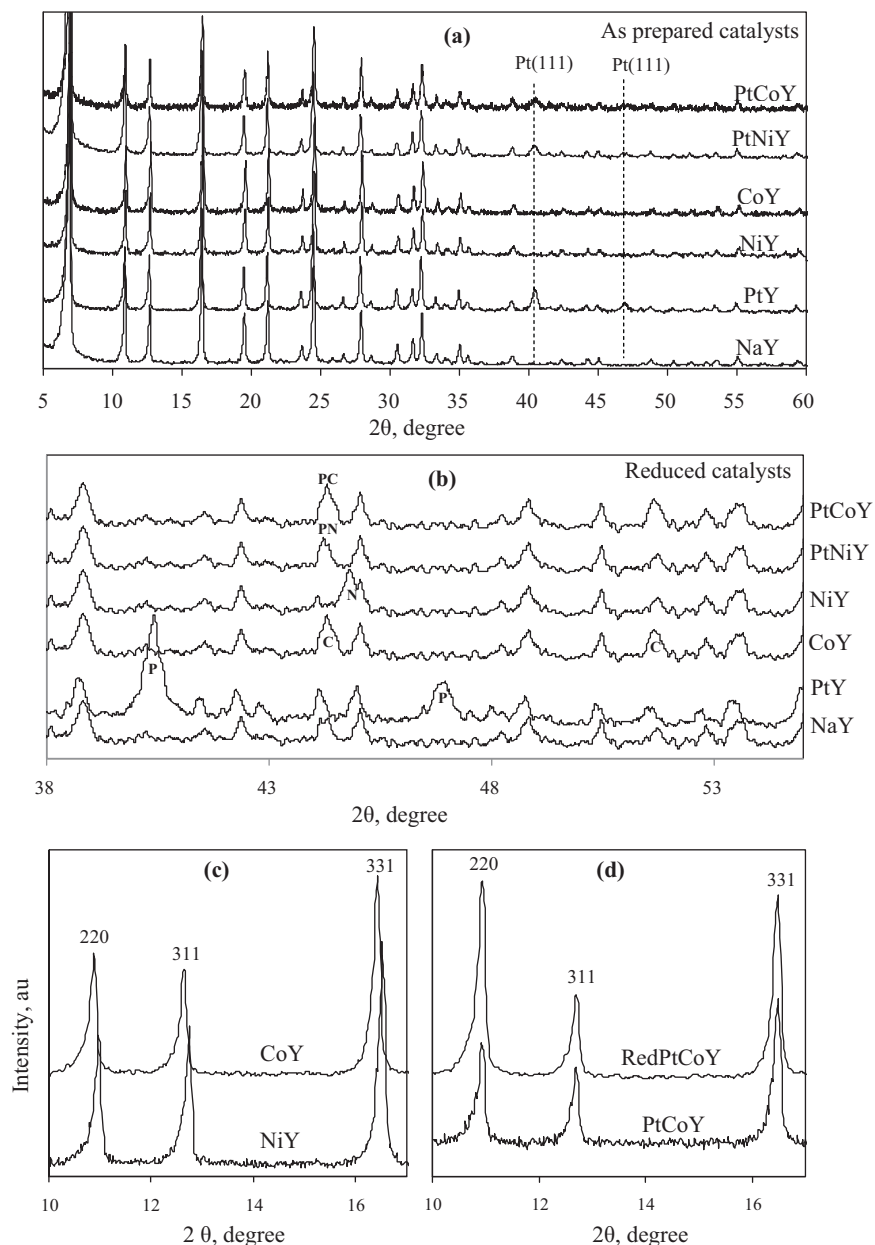


**Fig. 2.** Powder XRD patterns of parent NaY, as prepared and reduced catalysts. N = Ni<sup>0</sup>, C = Co<sup>0</sup>, PN = PtNi, PC = PtCo.

the reacting suspension was continuously magnetically stirred. To the mixture, unless otherwise stated, a sample weight of 20 mg of the employed catalyst was added and stirred at room temperature to be the zero time of the reaction ( $t_0$ ). The disappearance of 4-nitrophenolate dark yellow color was monitored using UV-vis spectrophotometer (Varian carry 50) by withdrawing 3 ml of mixture in different time intervals during the reaction. The solid suspension was separated from the solution by filtration and the quantitative determination of 4-nitrophenolate was performed by recording the absorption spectra at different time intervals. In agreement with previous literature [22–24], the kinetics of the reduction can be treated as pseudo-first order reaction with respect to 4-nitrophenol and applying the equation  $[\ln(C_0/C) = kt]$  where,  $C_0$  and  $C$  are the extinction of the peak maxima at 400 nm at the beginning of the reaction ( $t=0$ ) and after time  $t$ , respectively. The slope of the plot  $\ln(C_0/C)$  vs  $t(\text{min})$  gives the reaction rate constant ( $k$ ,  $\text{min}^{-1}$ ).

### 3. Results and discussions

#### 3.1. Characterization

##### 3.1.1. X-ray diffraction

The crystallinity of the prepared samples was confirmed by powder XRD analysis and all the measurements are shown in Fig. 2a. The patterns of parent NaY and the other prepared catalysts showed nine main lines at  $2\theta = 6.18^\circ$  (1 1 1),  $10.9^\circ$  (2 2 0),  $12.6^\circ$  (3 1 1),  $16.4^\circ$  (3 3 1),  $19.48^\circ$  (3 3 3),  $21.2^\circ$  (4 4 0),  $24.5^\circ$  (4 4 4),  $27.88^\circ$  (7 3 1) and  $32.32^\circ$  (8 4 0). Other small peaks at  $23.64^\circ$  (5 3 3),  $26.66^\circ$  (5 5 1),  $30.52^\circ$  (6 6 0),  $31.64^\circ$  (5 5 5),  $33.34^\circ$  (7 5 3),  $35.02^\circ$  (8 4 4),  $38.72^\circ$  (10 2 2),  $42.38^\circ$  (8 6 6),  $48.82^\circ$  (11 7 2),  $52.82^\circ$  (10 8 2),  $53.50^\circ$  (9 9 7) were also detected. According to the JCPDS powder diffraction database file [PDF# 38-0239], these XRD lines are typical to NaY zeolite which is also in a good agreement with previous literature [25,26]. These lines were observed in all the measured patterns

of all the samples. This indicates that the zeolitic structure ordering remains unchanged after incorporation of metal ions into NaY zeolite. The Pt containing sample showed small lines at  $2\theta = 40.4^\circ$  and  $47^\circ$  which are characteristic of Pt(1 1 1) and Pt(2 0 0) phases, respectively [PDF# 87-0647]. However, the patterns did not show any of Co or Ni oxides phases which may be due to the low concentration of Co and Ni oxides or the encapsulation of these oxides in the NaY zeolite cages.

The representative XRD patterns of the reduced Pt-free and Pt-promoted CoY and NiY catalysts are shown in Fig. 2b. The pattern of reduced NiY catalyst shows small diffraction peaks at  $2\theta = 44.5^\circ$  (1 1 1) and  $52^\circ$  (2 0 0) which correspond to cubic  $\text{Ni}^0$  [PDF# 88-2326]. Moreover, small peaks at  $2\theta = 46^\circ$  (1 1 1) and  $54^\circ$  (2 0 0) which correspond to  $\text{Co}^0$  [PDF# 88-2325] in the pattern of reduced CoY catalyst were observed. Small peak due to PtCo at  $2\theta = 44^\circ$  (1 1 1) [PDF# 43-1358] was detected in the catalyst containing platinum and cobalt. Furthermore, PtNi alloy may be detected at  $2\theta = 44.5^\circ$  in case of PtNiY catalyst. According to Ahmadi et al. [27] and Takenaka et al. [28], it is well acceptable to form PtCo alloys over Y zeolite after reduction with  $\text{H}_2$  gas at  $400^\circ\text{C}$ .

Quayle and Lunsford [29] reported that an empirical derived relationship exists between the relative 331, 311, and 220 peak intensities and cation location in faujasite type zeolites. If the intensities are in the order of  $I_{331} > I_{220} > I_{311}$ , the cations are randomly distributed within the lattice. However, if  $I_{331} > I_{311} > I_{220}$ , the cations assume positions at sites I<sup>-</sup> and II. Site I<sup>-</sup> is the sodalite cavity, while site II is at the center of a single six-ring (S6R) or displaced from this point into a supercage [30]. Using these empirical criteria, the diffraction patterns, Fig. 2c, suggest that the  $\text{Co}^{2+}$  is probably located in random positions while  $\text{Ni}^{2+}$  may be located at sites I<sup>-</sup> and II. However, after reduction of NiY, the Ni did not take specified sites (I<sup>-</sup> and II) and it is suggested that it is probably located in random positions. In case of bimetallic system, Fig. 2d shows that the ions in the unreduced sample PtCoY are randomly distributed while reduction directs the ions in specific positions since  $I_{220} > I_{331} > I_{311}$ .

The relative crystallinity was estimated by comparing the main peaks intensities with that of the parent NaY zeolite (100%). The relative crystallinity of the prepared samples decreased as summarized in Table 1. The Pt particle size was calculated by Scherrer's equation and it was found to be  $\approx 20$  and  $\approx 16$  nm in PtY and PtCoY, respectively, Table 1. This indicates that nanosized Pt particles are easily prepared by the employed method. The decrease in particle size in bimetallic system is in a good agreement with previous reports [3,7]. However, it was reported in literature that Pt particle size increased after addition of secondary metal prepared by incipient wetness [31,32] or vapor deposition [33] methods.

### 3.1.2. FTIR spectroscopy

IR spectra (not shown) of parent NaY zeolite and the Pt-promoted CoY and NiY catalysts in the range of  $4000\text{--}400\text{ cm}^{-1}$

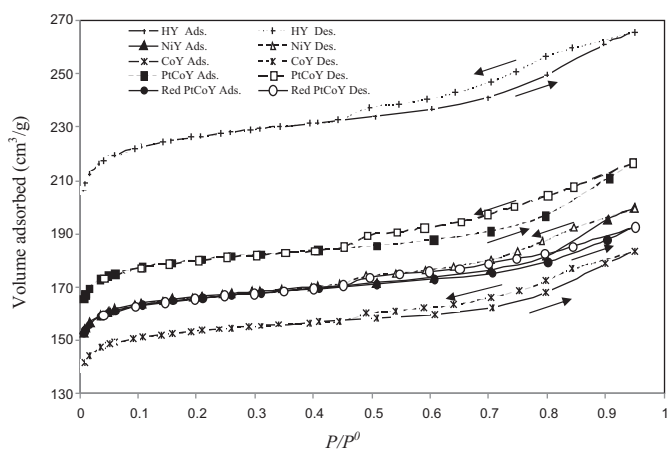


**Fig. 3.** Nitrogen adsorption-desorption isotherms for parent NaY and different metals loaded NaY catalysts.

exhibited broad peak centered at  $3440\text{ cm}^{-1}$  and other peak at  $1637\text{ cm}^{-1}$  which are attributed to stretching vibrations of surface hydroxyl groups and the absorption frequency of H—OH, respectively [34,35]. The spectra showed also peaks typical for Y zeolite at 1173, 1057, 823, 745, 589 and  $459\text{ cm}^{-1}$  [36]. The bands related to external linkages between  $\text{TO}_4$  tetrahedra and sensitive to the framework structure were observed at 1173, 823, and  $589\text{ cm}^{-1}$ . Moreover, the structural insensitive vibrations caused by internal vibrations of  $\text{TO}_4$  tetrahedra of NaY were observed at 1057, 745 and  $459\text{ cm}^{-1}$  [36]. As described in XRD patterns, FTIR data gave another verification that the structure of NaY zeolite is kept intact after incorporating of metal ions and calcination at  $500^\circ\text{C}$ . In coherence with XRD data, FTIR spectra did not show any peaks characteristic of M—O bonds which may be due to the low concentration of these oxides.

### 3.1.3. Surface texture characteristics of the prepared solids

The effect of incorporating metal ions to NaY zeolite on the surface adsorption capacity and pore structure can be clearly seen in the  $\text{N}_2$  sorption isotherms, Fig. 3. For the sake of clarity, some of the isotherms were omitted. According to the IUPAC classification, the isotherms of all the samples resembled type IV closely or faintly, suggesting the coexistence of mesopores and micropores [37]. The isotherms have relatively high adsorption below relative pressure ( $P/P_0$ ) of 0.1 due to micropore filling. With increasing nitrogen pressure (indicated by an arrow), a gradual increase in adsorption was observed up to  $P/P_0 = 0.7$ , and then followed by a sudden increase of adsorption until  $P/P_0 = 0.95$ . The overall adsorption was the highest in NaY zeolite ( $265\text{ cm}^3/\text{g}$ ) while it was the lowest in case of CoY ( $184\text{ cm}^3/\text{g}$ ). This is reflected in the specific surface area values ( $S_{\text{BET}}$ ) which are listed in Table 1. Overall, the porosity of

**Table 1**  
Physical properties of the prepared catalysts.

Catalyst	Crystallinity (%)	$S_{\text{BET}}$ ( $\text{m}^2/\text{g}$ )	Pore size cc/g	Pore radius ( $\text{\AA}$ )	Particle size <sup>a</sup> (nm)	Metal <sup>b</sup> (wt%)		
						Pt	Co	Ni
NaY	100	719	0.151	4.548	—	—	—	—
PtY	76	556	0.118	4.544	20	2.22	—	—
NiY	82	526	0.113	4.540	—	—	—	2.61
CoY	84	486	0.105	4.665	—	—	2.4	—
PtNiY	71	525	0.099	4.661	14	2.89	—	2.02
PtCoY	77	572	0.122	4.553	16	2.64	1.03	—
RedPtY	83	—	—	—	18	2.26	—	—
RedPtCoY	97	—	—	—	14	2.72	1.11	—

<sup>a</sup> Particle size calculated from TEM images.

<sup>b</sup> Weight ratio calculated from EDX.

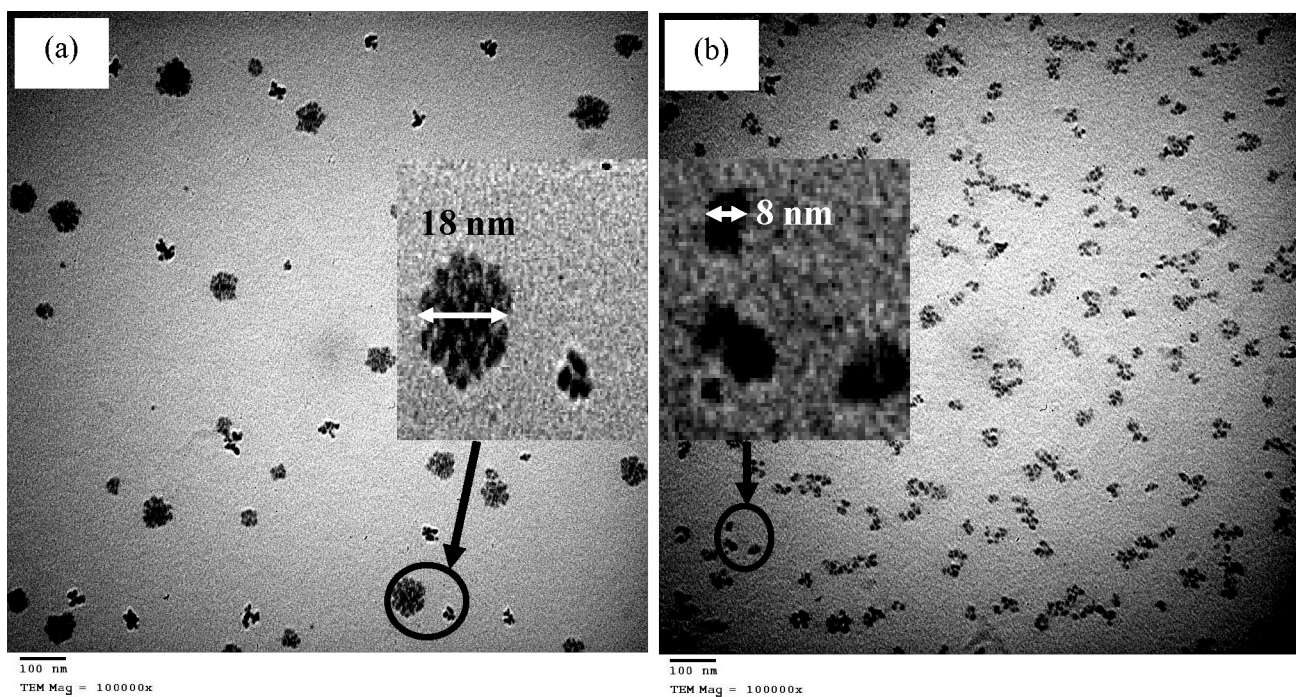


**Fig. 4.** TEM images of: (a) Co-free and (b) Co-promoted PtY catalysts.

these samples appears to be dominated by both micropores and mesopores, however, it decreased after addition of metal ions, as described by the decrease of pore volume and pore radius (**Table 1**). The presence of micropores is consistent with the zeolitic structural ordering as shown previously in XRD patterns. In all cases, the porosity was persisted even after preparation of monometallic or bimetallic systems.

#### 3.1.4. TEM micrographs

The TEM images of PtY and PtCoY are shown in **Fig. 4**. It is clearly presenting that the particle size of PtY was  $\approx 18$  nm, **Fig. 4a**. Significant morphological changes were obtained after promotion of CoY with platinum (PtCoY). The micrograph of PtCoY, **Fig. 4b**, showed that the particle size decreased to  $\approx 8$  nm. This indicates that the dispersion in PtCoY catalyst is more than that of Co-free PtY catalyst. This is in coherence with the data obtained from XRD patterns and in agreement with previous literature [3,7].

#### 3.1.5. EDX analysis

The EDX analysis of the prepared catalysts determined the amount of metal ions loaded on NaY zeolite. The data are summarized in **Table 1**. It showed that the ratio between Pt/Ni = 1.4 while the ratio of Pt/Co = 2.6. The difference between Pt/Co and Pt/Ni may be due to the difference in ion exchange ability and capacity between Na and Co or Ni ions.

#### 3.2. Catalytic reduction of 4-nitrophenol

The reduction of 4-NP over the prepared samples in the presence of NaBH<sub>4</sub> was previously investigated for the efficient production of 4-AP [21–24]. In addition to the previous important reason, this reaction was used as a model reaction to examine the effect of promotion with platinum on the catalytic performance of CoY and NiY catalysts. The results showed that the prepared samples efficiently assisted the catalytic reduction of 4-NP. Moreover, no hydrogenation reaction was observed without using catalyst. This confirms the absence of any noncatalytic reduction of 4-NP. Before investigating the catalytic activity of metal supported zeolite, NaY zeolite,

as expected, did not show any catalytic performance toward the reduction of 4-nitrophenol in the presence of NaBH<sub>4</sub>. Interestingly, after the addition of metal containing zeolite (PtCoY) to the solution (4-NP + NaBH<sub>4</sub>), there was a continuous fading of color until discoloration of solution. This was clear from the decrease of the peak located at 400 nm characteristic of 4-nitrophenolate, **Fig. 5**. Also, two new peaks at 295 and 230 nm due to 4-aminophenol (4-AP) increased with the time progress. It is noticed that, there is no proportional increase in the 4-aminophenol peak intensity with that of 4-nitrophenol; probably due to the difference in the molar extinction co-efficient of 4-nitrophenolate and 4-aminophenol [38]. The UV-vis spectra show an isosbestic point (315 nm), illustrating that the catalytic reduction of 4-NP yields only 4-AP without byproducts [17,39].

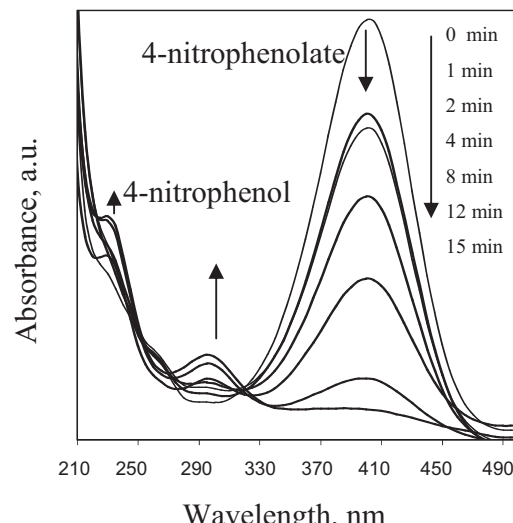


**Fig. 5.** Time-dependant UV-vis absorption spectral changes of the 4-NP reduction at 28 °C using 100 ml aqueous solution containing 20 mg PtCoY catalyst, 4-NP (0.72 mmol) and NaBH<sub>4</sub> (1.5 mmol).

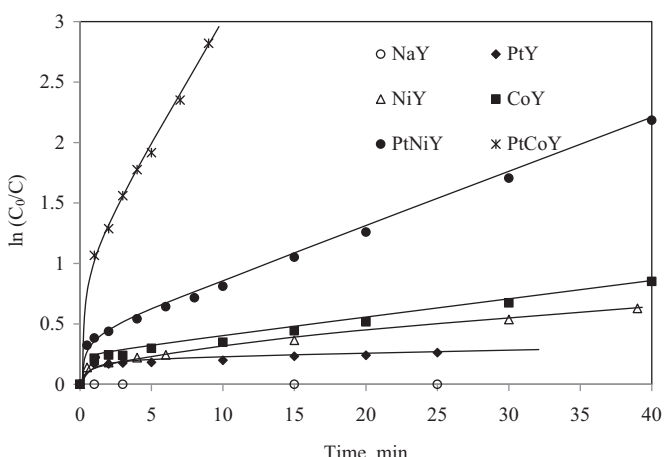


**Fig. 6.** Pseudo-first order plots of 4-NP reduction in the presence of  $\text{NaBH}_4$  over parent NaY and different metals loaded NaY catalysts at  $28^\circ\text{C}$  using 100 ml aqueous solution containing 20 mg catalyst, 4-NP (0.72 mmol) and  $\text{NaBH}_4$  (1.5 mmol).

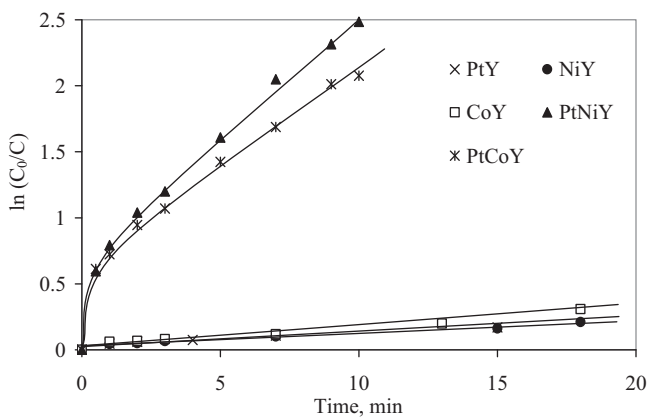
### 3.2.1. Reduction of 4-nitrophenol in the presence of different catalysts

Fig. 6 shows the pseudo-first order kinetics of 4-NP reduction in the presence of  $\text{NaBH}_4$  at  $28^\circ\text{C}$ . Straight lines were observed in the plots of  $\ln C_0/C$  vs  $t$  (min) after short period of time. During the first stage of the reaction, abrupt decrease in the concentration of 4-nitrophenolate ion was observed which may be due to the increase of  $\text{H}_2$  evolution in the first few seconds of reaction.

Although the dark yellow color of 4-nitrophenolate started to fade with time, the color still exists even after 60 min of reaction in case of simple metal oxides loaded on NaY zeolite (PtY, NiY and CoY). However, in Pt-promoted CoY and NiY systems (PtCoY and PtNiY), the fading of color was faster than that the case of supported simple oxide catalysts. Moreover, after using PtCoY, the color disappeared within 8 min of the reaction progress indicating its completion. The reaction rate constant values ( $k$ ,  $\text{min}^{-1}$ ) were calculated from the slope of the straight line portion and summarized in Table 2. It is clear that the catalytic performance was in the order of  $\text{PtY} < \text{NiY} < \text{CoY} < \text{PtNiY} < \text{PtCoY}$ . The  $k$  value ( $\text{min}^{-1}$ ) of 4-NP reduction at  $28^\circ\text{C}$  in the presence of PtCoY is 54 and 14 times more than that in the presence of PtY and CoY catalysts, respectively. Hence, the combination of Pt and Co greatly enhanced the catalytic activity toward the reduction reaction. Considering that all the metal atoms participate in the reaction to liberate  $\text{H}^+$  from  $\text{NaBH}_4$ , the ratio of 4-NP concentration (0.72 mmol) and the number of moles of metal atoms, measured by EDX, ( $[4\text{-NP}]/[\text{M}]$ ) was calculated and summarized in Table 2. It is clear that after completion of reaction, the turn over number of this reaction is 31.6, 8.3 and 12 in case of PtY, CoY and PtCoY catalysts, respectively.

In agreement with Ismail et al. [40], the careful inspection of the  $k$  ( $\text{min}^{-1}$ ) values, Table 2, showed that the catalytic activity did not have direct correlation with  $S_{\text{BET}}$ , pore diameter and pore volume, Table 1. However, the results indicated that the rate constants increased from  $4 \times 10^{-3} \text{ min}^{-1}$  to  $216 \times 10^{-3} \text{ min}^{-1}$  as the metal nanoparticle size decreased from 20 nm to 8 nm in PtY and PtCoY, respectively. It was reported that, in low particle size region, a decrease in the particle size leads to an increase in the fraction of low coordination metal sites such as vertices, edges, and kinks, which can promote adsorption of the reactants and facilitate the reaction [41].

The addition of platinum to either CoY or NiY leads to the formation of electron rich sites compared to those of PtY, CoY or NiY catalysts. Additionally, it decreases the acidic characters [3,7,42] of the surface of the catalyst. Lu et al. [43] reported that the activity of Ni-containing catalysts toward the hydrogenation of 4-NP

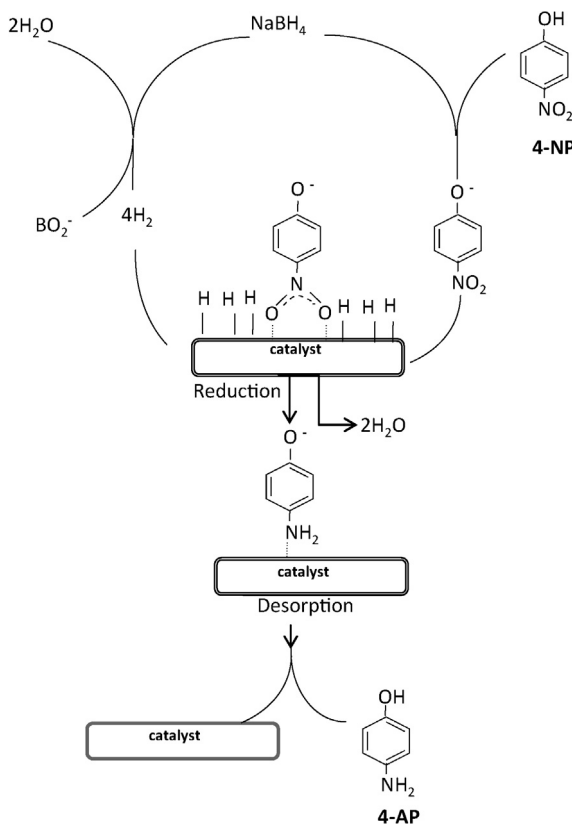


**Fig. 7.** Pseudo-first order plots of 4-NP reduction in the presence of  $\text{NaBH}_4$  over 5 mg of reduced catalysts at  $28^\circ\text{C}$  using 100 ml aqueous solution containing 4-NP (0.72 mmol) and  $\text{NaBH}_4$  (1.5 mmol).

increased in the presence of the reduced metallic Ni amounts. Moreover, the presence of Pt enhances the reduction of Ni cations and forms more metal particles [3,42]. The reduction of metal ions over Y zeolite may be the reason of increasing the catalytic activity in bimetallic catalysts, namely, PtCoY or PtNiY. The presence of the reduced forms of these metals facilitates the adsorption of reactants, electron transfer from catalyst to phenolate ion and desorption of the products. It will be interesting to investigate the reduction of 4-NP in the presence of the reduced catalysts (higher basic sites) and aqueous solution of  $\text{NaBH}_4$ .

### 3.2.2. Effect of catalyst reduction

Since the basic metallic sites are believed to play a great role in the reduction of 4-NP by  $\text{NaBH}_4$ , it is interesting to reduce the prepared catalysts and compare their catalytic activity toward the 4-NP hydrogenation reaction. Reduction of the catalysts was carried out using 80 Torr of pure  $\text{H}_2$  in static vacuum conditions at  $400^\circ\text{C}$  for 30 min and in the presence of liquid nitrogen trap. The catalytic activity of the reduced catalysts toward the reduction ( $4\text{-NP} \rightarrow 4\text{-AP}$ ) was tested and the reaction was too fast to follow when employing 20 mg catalyst. Therefore, the amount of catalyst was reduced to 5 mg while keeping other parameters unchanged. The first order plots of 4-NP reduction are presented in Fig. 7. The catalytic activity was compared by calculating the specific rate constant as  $k$  ( $\text{min}^{-1}$ )/mass (g) (Table 2). It is clear that the activity of the reduced catalysts is 8.5 and 3.7 times more than that of the unreduced ones in case of PtY and PtCoY, respectively, at  $28^\circ\text{C}$ . As mentioned in XRD data, it is expected to form PtCo and PtNi alloys over Y zeolite after reduction with  $\text{H}_2$  gas at  $400^\circ\text{C}$ . Kuroda et al. [16] reported that, the mechanism of the hydrogenation of nitro compound indicated that the process is influenced by factors such as proton availability and electron transfer to the nitro compound. Since the reaction is carried out in aqueous medium, protons are available and in excess. The relay of the electrons from the strong nucleophile  $\text{BH}_4^-$  (because of its diffusive nature and high electron injection capability) to the acceptor 4-NP via metal particles helps to overcome the kinetic barrier of the reaction and controls the reaction speed, Scheme 1. It can be noted that the presence of metallic form of the employed elements facilitates the relaying of electrons to 4-NP from borohydride ion to nitrophenolate ion. Similar data were obtained by other work groups when using  $\text{Ni}/\text{Al}_2\text{O}_3$ ,  $\text{Ni}/\text{TiO}_2$  [43] and  $\text{CuO}$  [44]. These data confirms the high activity of metallic particles in the hydrogenation of 4-NP to 4-AP which may be due to the ease of hydrogen adsorption over metallic sites and 4-AP desorption out of these sites. The greatest change in apparent rate constant was noticed for PtNiY which increased



**Scheme 1.** Proposed scheme of 4-NP reduction in presence of NaBH<sub>4</sub> and the prepared catalysts.

16 times after reduction whereas PtCoY increased 3.7 times after reduction. However, the rate constant of reduced PtCoY is the highest amongst the employed catalysts. Additionally, the turn over number increased to 114 and 47.6 in case of reduced PtY and PtCoY catalysts, respectively.

It is noteworthy to mention that, the apparent rate constant obtained for 4-NP reduction in the presence of reduced PtCoY

**Table 3**  
Comparison of apparent rate constants for 4-nitrophenol reduction over reduced PtCoY with different reported catalyst systems.

Catalyst	Apparent rate constant (min <sup>-1</sup> )	Reference
Ti/Al <sub>2</sub> O <sub>3</sub>	$3 \times 10^{-3}$	[45]
Pure Pt	$7.2 \times 10^{-3}$	[46]
Raney Ni	$9 \times 10^{-3}$	[38]
Ni–Pt (64:36)	$28.8 \times 10^{-3}$	[38]
Ni–Pt (20:80)	$54 \times 10^{-3}$	[38]
Microgel–Pd	$90 \times 10^{-3}$	[47]
Ni–Pt (94:6)	$115.8 \times 10^{-3}$	[38]
Red PtCoY	$201 \times 10^{-3}$	This work
PNIPA <sup>a</sup> gels (Ag)	$210 \times 10^{-3}$	[48]
PAMAM <sup>b</sup> –Pd	$215 \times 10^{-3}$	[20]
PAMAM <sup>b</sup> –Au	$222 \times 10^{-3}$	[49]
SPB <sup>c</sup> –Pd	$264 \times 10^{-3}$	[38]

<sup>a</sup> PNIPA denotes Poly(N-isopropylacrylamide).

<sup>b</sup> PAMAM denotes poly(amidoamine).

<sup>c</sup> SPB denotes Spherical Polyelectrolyte Brushes.

catalyst is rather high in comparison to almost all previous findings in the literature [20,45–49] including those obtained with Pt and Ni (Table 3).

### 3.2.3. Effect of mass of catalyst

As previously mentioned, the catalyst PtCoY exhibited the highest catalytic activity. Therefore, the effect of the amount of the catalyst PtCoY on the rate of 4-NP reduction was studied using different catalyst masses in the range of 5–50 mg while keeping the other parameters unchanged. Fig. 8a shows the pseudo-first order plots of 4-NP in the presence of NaBH<sub>4</sub> and different masses of PtCoY catalyst. As expected, an enhancement of the catalytic efficiency was noticed with increasing the amount of catalyst. The relation between the rate constant and the catalyst mass was found to be linear when using N-CMC and AuNPs [22,50]. Chen and Ray [51] showed that the catalytic activity gave limiting value at high catalyst concentration. On the other hand, the relation between catalyst mass and the catalytic activity showed a volcano shape in the photocatalytic degradation of 4-NP over Fe-MFI catalyst [52]. In the present work, the catalytic activity increased progressively in logarithmic relation with the increase of catalyst weight and the plot of log(*k*) vs the catalyst mass shows a linear relation, Fig. 8b.

**Table 2**  
4-NP reduction experiments over the prepared catalysts.<sup>a</sup>

Catalyst	Temperature (°C)	Mass (mg)	$10^{-3} \times k$ (min <sup>-1</sup> )	$K_{sp}$ (min <sup>-1</sup> g <sup>-1</sup> )	$E_a$ (kJ/mol)	[4-NP]/[M]
PtY	28	20	4	0.2 0.665 1.61	136	31.6
	35	20	13.3			
	40	20	32.2			
NiY	28	20	12	0.6 1.75 3.05	105	28
	35	20	35			
	40	20	61			
CoY	28	20	16	0.8 1.45 2	60	8.3
	35	20	29			
	40	20	40			
PtNiY	28	20	47	2.35 6.3 14.85	119	7.2
	35	20	126			
	40	20	297			
PtCoY	28	20	216	10.8 17.3 25.15	55	12
	35	20	346			
	40	20	503			
Red PtY	28	5	8.7	1.7 3.8 6.6	117	114
	35	5	19			
	40	5	33			
Red CoY	28	5	11.5	2.3	–	–
Red NiY	28	5	8.4	1.6	–	–
Red PtNiY	28	5	193	38.6	–	–
Red PtCoY	28	5	201	40.2 73 119.8	48	47.6
	35	5	365			
	40	5	599			

<sup>a</sup> Reaction conditions: 100 ml aqueous solution containing 4-NP (0.72 mmol) and NaBH<sub>4</sub> (1.5 mmol); reaction temperature (28–40 °C); catalyst mass (5–20 mg).

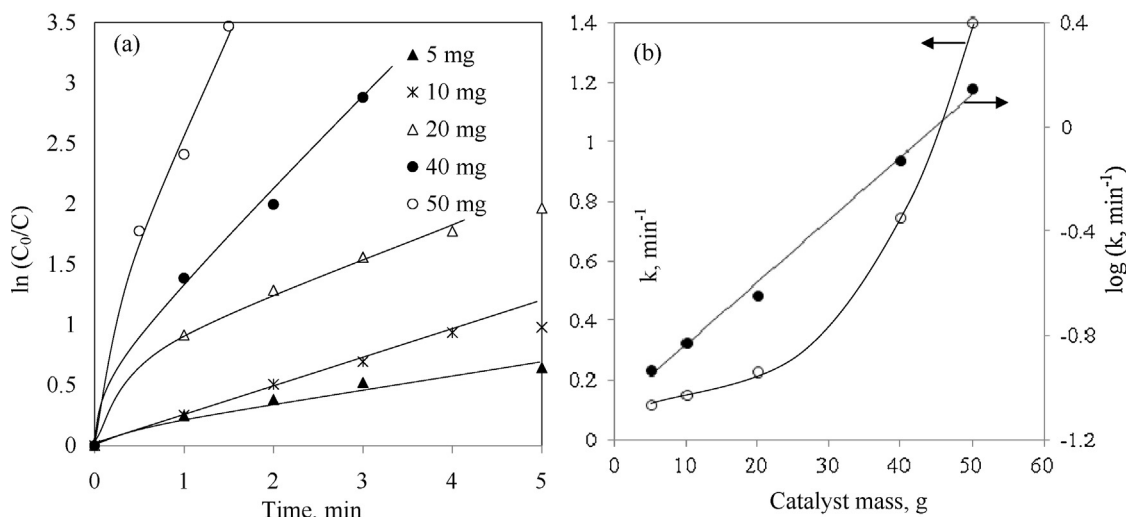


**Fig. 8.** (a) Pseudo-first order plots of the reduction of 4-NP in the presence of  $\text{NaBH}_4$  and different amounts of PtCoY catalyst at  $28^\circ\text{C}$  using 100 ml aqueous solution containing 4-NP (0.72 mmol) and  $\text{NaBH}_4$  (1.5 mmol); (b) the relationship between the rate constant ( $k, \text{min}^{-1}$ ) and the catalyst mass.

In addition, the turn over number increased to 114 and 47.6 after catalyst reduction in case of RedPtY and RedPtCoY, respectively. This refers to the ability of the prepared catalysts to complete the reaction even with relatively low metal concentration.

### 3.2.4. Effect of temperature

The effect of temperature on the pseudo-first order rate constant of the catalytic hydrogenation of 4-NP to 4-AP in the presence of  $\text{NaBH}_4$  and the different prepared catalysts was studied in the temperature range of  $28\text{--}40^\circ\text{C}$ . The activation energy values were calculated by using Arrhenius equation:

$$\ln k = \ln A - \left( \frac{E_a}{RT} \right) \quad (2)$$

where  $k$  is the rate constant,  $E_a$  is the apparent activation energy,  $R$  is the ideal gas constant ( $R=8.314 \text{ J K}^{-1} \text{ mol}^{-1}$ ) and  $T$  is the absolute temperature (K). The  $E_a$  was calculated from the slope of the plot ( $\ln k$  vs.  $1/T$ ), Fig. 9, and the data are summarized in Table 2. The highest activation energy (136 kJ/mol) was noticed for the 4-NP reduction in the presence of PtY catalyst, however,  $E_a$  decreased when using PtNiY and PtCoY to 119 and 56 kJ/mol, respectively. As expected,  $E_a$  of 4-NP hydrogenation in presence of reduced PtY

and PtCoY decreased to 117 and 48 kJ/mol, respectively, Table 2. The decrease of the activation energy of the hydrogenation reaction in presence of RedPtCoY indicates that the proceeding of the reaction over the reduced catalysts is more facile than that in case of unreduced catalysts. This strengthens the idea that, the presence of more basic sites in the catalyst surface increases the electron relay from  $\text{BH}_4^-$  to 4-NP and reaction becomes easier.

## 4. Conclusions

In conclusion, reactive and efficient Pt-promoted CoY and NiY catalysts were successfully prepared by successive ion exchange method. They were used for the catalytic reduction of 4-nitrophenol to 4-aminophenol with high catalytic performance. Taking PtY catalyst as a reference (the least  $K$  value), the relative catalytic performance calculated from the specific rate constant values ( $K_{sp}(\text{catalyst})/K_{sp}(\text{PtY})$ ) was in the order of PtY(1) < NiY(3) < CoY(4) < RedNiY(8) < RedPtY(8.5) < RedCoY(11.5) < PtNiY(11.7) < PtCoY(54) < RedPtNiY(193) < RedPtCoY(201). Meanwhile, the apparent activation energy was the highest in case of PtY (136 kJ/mol) while it decreased to  $\approx 1/3$  of this value in the case of RedPtCoY catalyst. The experimental data showed that, the presence of low oxidation states or metallic forms on the catalyst surface has an important role in the catalytic reduction of 4-NP.

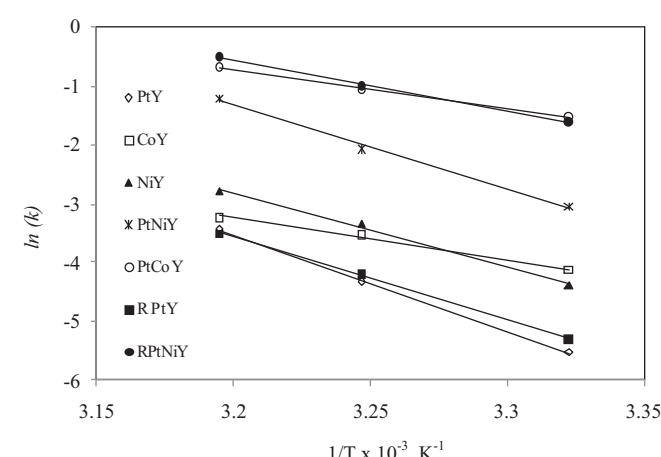
## Appendix A. Supplementary data

Supplementary data associated with this article can be found, in the online version, at <http://dx.doi.org/10.1016/j.apcata.2013.08.047>.

## References

- [1] P. Chin, X. Sun, G.W. Roberts, J.J. Spivey, *Appl. Catal. A* 302 (2006) 22–31.
- [2] C. Kwak, T.J. Park, D.J. Suh, *Appl. Catal. A* 278 (2005) 181–186.
- [3] M.H. Jordão, V. Simões, D. Cardoso, *Appl. Catal. A* 319 (2007) 1–6.
- [4] P.M. Lima, T. Garetto, C.L. Cavalcante, D. Cardoso, *Catal. Today* 172 (2011) 195–202.
- [5] L.R. Radhi de Araujo, M. Schmal, *Appl. Catal. A* 235 (2002) 139–147.
- [6] X. Liu, O. Korotkikh, R. Farrauto, *Appl. Catal. A* 226 (2002) 293–303.
- [7] Z.M. El-Bahy, A.I. Hanafy, M.M. Ibrahim, M. Ampo, *J. Mol. Catal. A* 344 (2011) 111–121.
- [8] N. Calace, E. Nardi, B.M. Petronio, M. Pietroletti, *Environ. Pollut.* 118 (2002) 315–319.
- [9] F. Akbal, O. Nur, *Environ. Monit. Assess.* 83 (2003) 295–302.

**Fig. 9.** Arrhenius plots ( $\ln k - 1/T$ ) for 4-NP reduction in the presence of different catalysts in the range of  $28\text{--}40^\circ\text{C}$  using 100 ml aqueous solution containing 4-NP (0.72 mmol),  $\text{NaBH}_4$  (1.5 mmol) and 20 mg of the as prepared catalysts or 5 mg of the reduced catalysts.



- [10] K.S. Yun, B.W. Cho, Process for preparing para-aminophenol, US Patent 5,066,369 (1991).
- [11] T. Komatsu, T. Hirose, *Appl. Catal. A* 276 (2004) 95–102.
- [12] M.J. Vaidya, S.M. Kulkami, R.V. Chaudhari, *Org. Process Res. Dev.* 7 (2003) 202–208.
- [13] C.M. Kaufman, B. Sen, *J. Chem. Soc. Dalton Trans.* (1985) 307–313.
- [14] Y. Kojima, K. Suzuki, K. Fukumoto, M. Sasaki, T. Yamamoto, Y. Kawai, H. Hayashi, *Int. J. Hydrogen Energy* 27 (2002) 1029–1034.
- [15] C. Wu, H. Zhang, B. Yi, *Catal. Today* 93–95 (2004) 477–483.
- [16] K. Kuroda, T. Ishida, M. Haruta, *J. Mol. Catal. A* 298 (2009) 7–11.
- [17] X. Du, J. He, J. Zhu, L. Sun, S. An, *Appl. Surf. Sci.* 258 (2012) 2717–2723, references mentioned elsewhere.
- [18] P. Klug, L.E. Alexander, *Direction Procedures for Polycrystalline and Amorphous Materials*, Wiley, New York, 1954.
- [19] S. Manivannan, B. Krishnakumari, R. Ramaraj, *Chem. Eng. J.* 204–206 (2012) 16–22.
- [20] K. Esumi, R. Isono, T. Yoshimura, *Langmuir* 20 (2004) 237–243.
- [21] S. Praharaj, S. Nath, S.K. Ghosh, S. Kundu, T. Pal, *Langmuir* 20 (2004) 9889–9892.
- [22] Z.M. El-Bahy, K.H. Mahmoud, *Spectrochim. Acta A* 92 (2012) 105–112.
- [23] C.H. Chiou, C.Y. Wu, R.S. Juang, *Sep. Purif. Technol.* 62 (2008) 559–564.
- [24] S. Arora, P. Kapoor, M.L. Singla, *React. Kinet. Mech. Catal.* 99 (2010) 157–165.
- [25] P.M. Barata-Rodrigues, T.J. Mays, G.D. Moggridge, *Carbon* 41 (2003) 2231–2246.
- [26] M.M.J. Treacy, J.B. Higgins, *Collection of Simulated XRD Powder Patterns for Zeolites*, fifth ed., Elsevier, New York, 2007.
- [27] R. Ahmadi, M.K. Amini, J.C. Bennett, *J. Catal.* 292 (2012) 81–89.
- [28] S. Takenaka, A. Hirata, E. Tanabe, H. Matsune, M. Kishida, *J. Catal.* 274 (2010) 228–238.
- [29] W.H. Quayle, J.H. Lunsford, *Inorg. Chem.* 21 (1982) 2226–2231.
- [30] M.N. Bae, M.K. Song, Y. Kim, *Bull. Korean Chem. Soc.* 22 (2001) 1081–1088.
- [31] A. Sirijaruphan, J.G. Goodwin, R.W. Rice Jr., *J. Catal.* 221 (2004) 288–293.
- [32] A. Sirijaruphan, J.G. Goodwin Jr., R.W. Rice, *J. Catal.* 224 (2004) 304–313.
- [33] S.K. Jain, E.M. Crabb, L.E. Smart, D. Thompsett, A.M. Steele, *Appl. Catal. B* 89 (2009) 349–355.
- [34] S. Guerrero, J.T. Miller, A.J. Kropf, E.E. Wolf, *J. Catal.* 262 (2009) 102–110.
- [35] Y. Zang, R. Farnood, *Appl. Catal. B* 79 (2008) 334–340.
- [36] R. Cid, F.J.G. Llambías, J.L.G. Fierro, A.L. Agudo, J. Villaseñor, *J. Catal.* 89 (1984) 478–488.
- [37] M. Kruck, M. Jaroniec, *Chem. Mater.* 13 (2001) 3169–3183.
- [38] S. Harish, J. Mathiyarasu, K.L.N. Phani, V. Yegnaraman, *Catal. Lett.* 128 (2009) 197–202.
- [39] Y. Deng, Y. Cai, Z.K. Sun, D.Y. Zhao, *J. Am. Chem. Soc.* 132 (2010) 8466–8473.
- [40] A.A. Ismail, A. Hakki, D.W. Bahnemann, *J. Mol. Catal. A* 358 (2012) 145–151.
- [41] G.A. Somorjai, *Introduction to Surface Chemistry and Catalysis*, Wiley, New York, 1994.
- [42] I. Eswaramoorthi, N. Lingappan, *Catal. Lett.* 87 (2003) 133–142.
- [43] H. Lu, H. Yin, Y. Liu, T. Jiang, L. Yu, *Catal. Commun.* 10 (2008) 313–316.
- [44] T.R. Mandlimath, B. Gopal, *J. Mol. Catal. A* 350 (2011) 9–15.
- [45] V. Loddo, G. Marci, L. Palmisano, A. Scalfani, *Mater. Chem. Phys.* 53 (1998) 217–224.
- [46] S.K. Ghosh, M. Mandal, S. Kundu, S. Nath, T. Pal, *Appl. Catal. A* 268 (2004) 61–66.
- [47] Y. Mei, Y. Lu, F. Polzer, M. Ballauff, M. Drechsler, *Chem. Mater.* 19 (2007) 1062–1069.
- [48] Y. Lu, Y. Mei, M. Drechsler, M. Ballauff, *Angew. Chem. Int. Ed.* 45 (2006) 813–816.
- [49] K. Hayakawa, T. Yoshimura, K. Esumi, *Langmuir* 19 (2003) 5517–5521.
- [50] K.B. Narayanan, N. Sakthivel, J. Hazard. Mater. 189 (2011) 519–525.
- [51] D. Chen, A.K. Ray, *Water Res.* 32 (1998) 3223–3234.
- [52] I.O. Ali, A.M. Ali, S.M. Shabaan, K.S. El-Nasser, *J. Photochem. Photobiol. A* 204 (2009) 25–31.